COMMUNICATION

Elucidating the coordination chemistry of the radium ion for targeted alpha therapy

Received 00th January 20xx,
Accepted 00th January 20xx

DOI: 10.1039/x0xx00000x

Alexander S. Ivanov,*[a] Megan E. Simms,[a] Vyacheslav S. Bryantsev,[a] Paul D. Benny,[b] Justin R. Griswold,[b] Laetitia H. Delmau,[b] Nikki A. Thiele*[a]

The coordination chemistry of Ra^{2+} is poorly defined, hampering efforts to design effective chelators for ^{223}Ra-based targeted alpha therapy. Here, we report the complexation thermodynamics of Ra^{2+} with the biomedically-relevant chelators DOTA and macropa. Our work reveals the highest affinity chelator to date for Ra^{2+} and advances our understanding of key factors underlying complex stability and selectivity for this underexplored ion.

Recently, there has been a surge of interest in radium (Ra) for targeted alpha (α) therapy (TAT), a rising cancer treatment strategy that couples the cytotoxicity of α particles with the tumor specificity of biological targeting vectors to selectively eradicate cancer cells.[1] This interest is spurred by the clinical success of the α emitter ^{223}Ra ($t_{1/2}$ = 11.43 d) for treating bone metastases in patients with castration-resistant prostate cancer.[2] Administered as a simple dichloride salt, $^{223}Ra^{2+}$ accumulates in bone because of its chemical similarity to endogenous Ca^{2+}, where it deposits a lethal dose of ionizing radiation. However, to advance this α emitter forward for TAT of non-osseous cancers, its stable attachment to a targeting vector via a bifunctional chelator is required.[3] Despite several efforts towards this goal,[4] no chelator has been found to complex ^{223}Ra with sufficient in vivo stability to enable its targeted delivery to soft-tissue metastases.

A key challenge hindering the development of suitable chelators for ^{223}Ra resides in our limited understanding of the coordination chemistry of Ra^{2+}, the largest +2 ion in the Periodic Table.[5] In this regard, even the most fundamental properties of Ra^{2+} in aqueous solution, such as the hydration number and bond distances of the Ra–aquo ion, remain unknown. Furthermore, few efforts have been undertaken to characterize the structure, kinetics, and thermodynamics of coordination complexes of Ra^{2+} with organic chelators.[6] As such, the key bonding interactions, association/dissociation mechanisms, and chemical speciation underlying the formation of (un)stable complexes of Ra^{2+} are poorly established. This information is challenging to obtain because of the limited availability and high radioactivity of all Ra isotopes. However, advancing our knowledge of these facets of Ra^{2+} coordination chemistry is critical for establishing a foundation upon which to build increasingly effective chelators for ^{223}Ra-based TAT.

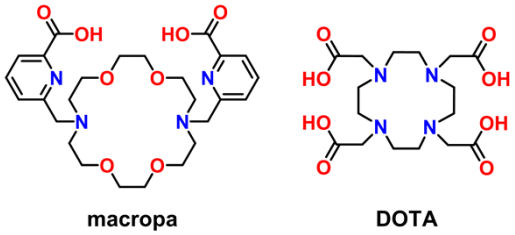

Fig. 1. Chemical structures of the chelators discussed in this work.

Towards this goal, we report our experimental and computational efforts to establish the complexation thermodynamics of Ra^{2+} with the macrocycles macropa and DOTA, two state-of-the-art chelators for TAT (Fig. 1). Through this work, we have discovered that macropa possesses the highest affinity reported to date for Ra^{2+} under physiologically relevant conditions. We also establish a better understanding of the bonding interactions and structural factors that underpin Ra^{2+} complex stability and selectivity. Our findings highlight how thermodynamic parameters coupled with atomic-level insights from quantum chemical calculations can be leveraged to establish ligand design principles for underexplored radioactive ions and mark an important step towards establishing the chelation chemistry of Ra^{2+}.

Our motivation for probing the complexation thermodynamics of Ra^{2+} with macropa and DOTA arises from their demonstrated ability to chelate similar radiometals of interest for nuclear medicine applications,[7] including the large $^{225}Ac^{3+}$ ion, another promising α emitter under investigation for TAT.[8] Furthermore, studies have shown that macropa and DOTA can bind the Ra^{2+} ion in aqueous solution,[4b,4d] sparking investigations into their use in ^{223}Ra-based TAT.[4d,9] However,

[a] *Chemical Sciences Division, Oak Ridge National Laboratory, Oak Ridge, Tennessee 37831, United States. E-mail: ivanova@ornl.gov, thielena@ornl.gov*
[b] *Radioisotope Science and Technology Division, Oak Ridge National Laboratory, Oak Ridge, Tennessee 37831, United States*

‡Electronic Supplementary Information (ESI) available: [details of radioisotopes, pH-potentiometric titrations, cation exchange and solvent extraction methods, and DFT calculations]. See DOI: 10.1039/x0xx00000x

despite this interest in macropa and DOTA for ^{223}Ra chelation, the stability constants, or log *K* values, of their complexes with Ra^{2+} remain unknown. These values can provide valuable insight into the fundamental coordination preferences of Ra^{2+} and serve as a useful metric to compare binding strengths and selectivities among chelators. To date, stability constant studies of Ra^{2+} complexes have been limited to simple organic acids and acyclic polyaminocarboxylate ligands,[6,10] which are known to form complexes of low stability in vivo with many radiometals.[7a] Here, we expand our knowledge of the stability constants of Ra^{2+} complexes to include two chelators that are directly relevant for use in biomedical applications. All experiments were carried out using ^{223}Ra as the source of the Ra^{2+} ion.

We first explored a biphasic competitive complexation method for determining $^{223}Ra^{2+}$ stability constants because it has been used previously to measure the stability constants of macropa with other radiometals.[11] However, we discovered unexpectedly that the neutral [Ra(macropa)] complex partitions to the organic phase (Fig. S1, ESI‡), rendering this method unsuitable for further use (Section 1.4, ESI‡). Instead, Ra^{2+} stability constants were measured via cation exchange with Dowex 50W X8 Na^+ resin[10a,12] and an aqueous phase comprising macropa or DOTA in MES or HEPES buffer, respectively. The ionic strength was held constant at 0.2 M with NaCl, a physiologically relevant electrolyte. From the resin/aqueous phase distribution ratios of ^{223}Ra in the absence (D_0) or presence (D) of varying concentrations of macropa and DOTA at a constant p[H], an overall conditional stability constant, or β_{app} value, for the complexation of Ra^{2+} by each ligand was obtained via linear regression according to eq (1).

$$\frac{D_0}{D} - 1 = \beta_{app}[L^{n-}] \qquad (1)$$

In this equation, $[L^{n-}]$ represents the concentration of fully deprotonated ligand, macropa^{2-} or DOTA^{4-}, which was calculated from $[L]_{total}$, solution p[H], and ligand protonation constants determined by potentiometric titration in 0.2 M NaCl (Table S1, Fig. S2–S6, ESI‡). β_{app} represents the sum of $\beta_{mhl}[H^+]^h$, wherein β_{mhl} is the stability constant for the complex MH_hL (Section 1.5.4, ESI‡).[13] A ligand-to-metal stoichiometry of 1:1 was determined for both chelators from slope analyses of logarithmic plots of the distribution data (Fig. S7–S8, Tables S2–S3, ESI‡). Analysis of β_{app} as a function of p[H] revealed the absence of protonated metal–ligand complexes over the p[H] range studied for each ligand (macropa, p[H] 5.62–6.29; DOTA, p[H] 7.68–8.46; Fig. S9–S17, ESI‡).[14] As such, the average log β_{app} value was taken as the pH-independent stability constant, or log K_{ML} value, for each $[Ra(L)]^n$ complex (Table S4, ESI‡).

Shown in Table 1, a log K_{RaL} value of 10.00(2) was determined for [Ra(macropa)]. This stability constant exceeds the largest published stability constant for a Ra^{2+} complex in aqueous solution, that of [Ra(diethylenetriaminepentaacetic acid)]$^{3-}$, by 1.5 orders of magnitude (log K_{RaDTPA} = 8.5, 0.1 M $NaClO_4$).[10c] By contrast, our results indicate that $[Ra(DOTA)]^{2-}$ is only moderately stable, reflected by a log K_{RaL} value of 7.82(4). This comparatively lower stability can be attributed to DOTA's high affinity for the Na^+ ion (log K_{NaDOTA} = 4.2),[15] which was used as part of the ionic medium and thermodynamically competes with Ra^{2+} for binding to DOTA. Conversely, Na^+ binding by macropa is negligible (Fig. S6, ESI‡). Upon further refinement of the data to account for Na^+ chelation by DOTA (Section 1.5.5, ESI‡), a log K_{RaL} value of ~11.3 was obtained, revealing DOTA's high affinity for the Ra^{2+} ion under Na^+-free conditions. This finding corroborates our current understanding of the nature of ligand binding interactions with the Ra^{2+} ion as being dominated by electrostatics, such that highly charged chelators like DOTA^{4-} are expected to form complexes of relatively high thermodynamic stability with Ra^{2+}.[6] However, these results also underscore the importance of considering the effects of Na^+ and other competing endogenous ions on Ra^{2+} complex stability when seeking to implement new chelators for ^{223}Ra-based TAT.

Table 1. Thermodynamic Stability Constants of Alkaline Earth Complexes of Macropa and DOTA Determined at 25 °C and I = 0.2 M NaCl[a]

	macropa^{2-}	DOTA^{4-}
log K_{CaL}	6.06(3)[b]	13.68(3)[b]
log K_{SrL}	9.70(1)[b]	11.81(4)[b]
log K_{SrHL}	3.35(4)[b]	
log K_{BaL}	11.45(3)[b], 11.02(7)[c]	9.31(3)[b], 9.46(2)[c]
log K_{BaHL}	3.74(1)[b]	
log K_{BaH2L}	2.79(7)[b]	
log K_{RaL}	10.00(2)[c,d]	7.82(4)[c,d]
log K'_{RaL}[e]	9.28	4.29

[a]The values in parentheses are 1 standard deviation of the last significant figure. [b]Determined via potentiometric titration. [c]Determined via ^{133}Ba or ^{223}Ra cation exchange. [d]No protonated ML complexes were detected over the pH range investigated (see text). [e]Conditional stability constant at p[H] 7.4.

In further comparing the complexation thermodynamics of macropa and DOTA with Ra^{2+}, another useful metric is provided by the conditional stability constant, or log *K*′ value, at physiological pH 7.4. This constant accounts for competition between protons and metals for binding to a ligand in aqueous solution, providing a more meaningful comparison of complex stability between chelators of differing basicities.[16] Notably, the log $K'_{pH7.4}$ value of [Ra(macropa)] is 9.28, only 0.72 log *K* units lower than the pH-independent log K_{ML} of the complex (Table 1). This retention of high affinity near neutral pH arises from macropa's low basicity ($\sum$log K_a = 20.6), such that a significant portion of the ligand is already completely deprotonated at pH 7.4. By contrast, $[Ra(DOTA)]^{2-}$ is destabilized by over 3 orders of magnitude at pH 7.4 (log $K'_{pH7.4}$ = 4.29). A log $K'_{pH7.4}$ value of 4.3 is also calculated for $[Ra(DOTA)]^{2-}$ under Na^+-free conditions. This dramatic pH-dependent decrease in complex stability is a consequence of DOTA's higher basicity ($\sum$log K_a = 28.9 and 32.4 in 0.2 M NaCl and NMe_4Cl, respectively). Collectively, these differences render [Ra(macropa)] 100,000-times more thermodynamically stable than $[Ra(DOTA)]^{2-}$ at pH 7.4, revealing macropa to be remarkably superior to DOTA for Ra^{2+} chelation under biologically-relevant conditions.

To garner further insight into the binding selectivities of macropa and DOTA in the context of Ra^{2+} chelation, we next determined the stability constants of their complexes with other alkaline earth (AE) ions, namely Ca^{2+}, Sr^{2+}, and Ba^{2+}, by potentiometric titration (Table 1, Fig. S2–S5, ESI‡). Ba^{2+} stability constants were also measured by cation exchange using ^{133}Ba

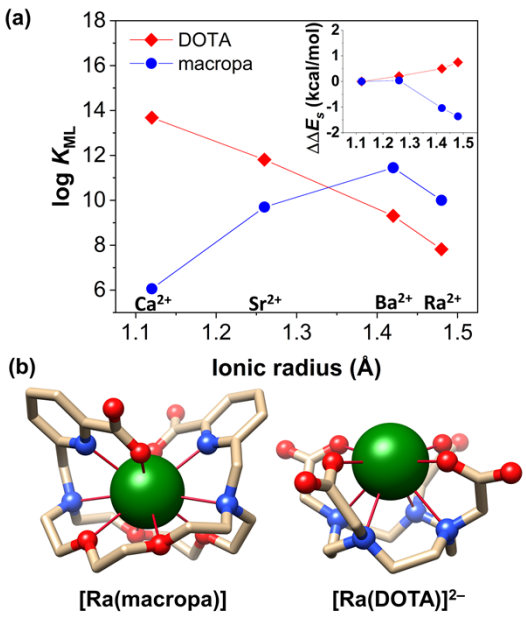

Fig. 2. (a) AE^{2+} stability constants of macropa and DOTA in 0.2 M NaCl versus the 8-coordinate ionic radius of each ion. Inset: Strain energies ($\Delta\Delta E_s$) of D18C6 and cyclen fragments of macropa and DOTA upon complexation with AE^{2+}, relative to Ca^{2+}. (b) DFT-optimized structures of [Ra(macropa)] and [Ra(DOTA)]$^{2-}$.

(Table 1, Fig. S18–22, ESI‡). The log K_{BaL} values from both techniques were similar, validating the accuracy of our radiotracer method. As shown in Fig. 2a, the affinity of DOTA for AEs steadily decreases in traversing down the group from the small Ca^{2+} ion (log K_{CaL} = 13.68) to the large Ra^{2+} ion (log K_{RaL} = 7.82). This trend is expected based on the conventional metal-ion selectivity pattern established for DOTA, in which smaller, more charge-dense ions are more strongly chelated in comparison to larger, less charge-dense ions.[15,17] By contrast, the stability constants of macropa with the AEs increase from Ca^{2+} (log K_{CaL} = 6.06) to Ba^{2+} (log K_{BaL} = 11.45). This unique preference for large over small metal ions has been previously reported for macropa and is attributed to a size match between large ions and the large 18-membered macrocyclic binding cavity of macropa.[18] However, unexpectedly, macropa complex stability drops by nearly 1.5 log K units on moving from the large Ba^{2+} ion to the even larger Ra^{2+} ion (Fig. 2a). This decrease in stability suggests that macropa's diaza-18-crown-6 (D18C6) macrocyclic cavity does not optimally stabilize Ra^{2+},[10d] revealing a limit in its effectiveness for binding large metal ions.

To gain a deeper understanding of the molecular origins of the obtained experimental results, we carried out density functional theory (DFT) calculations at the B3LYP/SC/def2TZVPP/IEF level of theory (see ESI‡ for details). We first validated our computational model by calculating the Gibbs free energy of exchange, $\Delta\Delta G^{calc}_{aq}$, for the competitive complexation of Ca^{2+} over larger AE^{2+} ions shown in eq. (2),

$$[Ca(NO_3)_2(H_2O)_{10}]_{(aq)} + [AE(L)]^n{}_{(aq)} \rightleftharpoons [Ca(L)]^n{}_{(aq)} + [AE(NO_3)_2(H_2O)_{10}]_{(aq)}, \Delta\Delta G^{calc}{}_{aq} \quad (2)$$

We have used this approach previously to predict ligand selectivities for f-block metal ions in aqueous medium.[19] The obtained $\Delta\Delta G^{calc}_{aq}$ values capture the AE selectivity trends of macropa and DOTA observed experimentally, in which macropa preferentially binds larger AE^{2+} ions over Ca^{2+}, giving rise to positive Ca/AE ΔΔG values, whereas DOTA forms more stable complexes with smaller cations, leading to negative Ca/AE ΔΔG values (Table 2). Impressively, our results are also in near quantitative agreement with $\Delta\Delta G^{exp}_{aq}$ values. Collectively, these data validate our computational model and demonstrate, for the first time, the accurate prediction of ligand selectivities for Ra^{2+} relative to other AE^{2+} metal ions.

Examination of the DFT-optimized geometries of [Ra(macropa)] and [Ra(DOTA)]$^{2-}$ (Fig. 2b) shows that Ra–O_e (O_e = ether oxygen) and Ra–N_a (N_a = amine nitrogen) bonds are typically ~0.4–0.5 Å longer than Ra–O_c (O_c = carboxylate oxygen) bond distances in the complexes. These differences suggest that the negatively charged pendent carboxylate donors of macropa and DOTA interact more strongly with Ra^{2+} than do the neutral macrocyclic ether and amine donors. To further probe these interactions, we performed natural bond orbital (NBO) analysis of chemical bonding in the complexes. As expected, the calculated Wiberg bond indices (WBIs, Table S6, ESI‡), which serve as a measure of bond order, are higher for Ra–O_c bonds (0.0378–0.0432) than for Ra–O_e and Ra–N_a bonds (0.0133–0.0199). [Ra(macropa)] is further stabilized by two Ra–N_p interactions with the pyridine nitrogen atoms, which also show comparatively high WBIs of 0.0285 due to partial delocalization of negative charge through conjugation with the carboxylate groups of macropa. Additionally, the NBO analysis indicates that the formal polarized Ra–O and Ra–N dative bonds originate from a characteristic σ-type donation of electron density from the donor O and N lone pairs (LP:) to the vacant acceptor orbitals (n^*_{Ra}) of primarily 7s character on Ra (Table S7, ESI‡). Collectively, these results support the notion that bonding interactions between Ra^{2+} and the chelators are predominately ionic in nature and underscore the importance of negatively charged donor atoms in stabilizing this ion.

Lastly, to understand the factors underpinning the trends in selectivity of macropa and DOTA for Ra^{2+} versus other AEs, we performed a second-order perturbation theory (SOPT) analysis coupled with relative strain energy ($\Delta\Delta E_s$) calculations. These studies correspondingly assess the strength of coordinate bonding interactions in the complexes and the ligand reorganization energy required for complexation. $\Delta\Delta E_s$ calculations were carried out for the neutral cyclen and D18C6 fragments of DOTA and macropa, respectively, to avoid bias from intraligand electrostatics (see Section 1.6, ESI‡). Second-order stabilization energies ($E^{(2)}$) for DOTA complexes were found to decrease from Ca^{2+} to Ra^{2+} (Table S7, ESI‡), reflecting less delocalization of LP:→n^*_{AE} dative bonds towards the AE center with increasing size, and thus decreasing charge density, of the metal ion. Synergistic with these results, $\Delta\Delta E_s$ values increase for cyclen with increasing AE ionic radius (Fig. 2a inset), which is consistent with the 12-membered macrocyclic cavity of DOTA being preorganized for binding small, but not large, metal ions. By contrast, D18C6 exhibits a general decrease in $\Delta\Delta E_s$ down the AE series (Fig. 2a inset), suggesting that macropa's 18-membered macrocyclic cavity is more suitable for binding larger metal ions. However, this favourable structural reorganization

Table 2. Experimental ($\Delta\Delta G^{exp}_{aq}$) and calculated ($\Delta\Delta G^{calc}_{aq}$) Gibbs free energies (kcal/mol) for the reaction given by Equation (2).

		Ca^{2+}/Sr^{2+}	Ca^{2+}/Ba^{2+}	Ca^{2+}/Ra^{2+}
macropa	$\Delta\Delta G^{exp}_{aq}$	4.96	7.35	5.37
	$\Delta\Delta G^{calc}_{aq}$	5.45	8.11	5.51
DOTA	$\Delta\Delta G^{exp}_{aq}$	–2.55	–5.96	–7.99
	$\Delta\Delta G^{calc}_{aq}$	–2.72	–4.64	–8.18

of macropa upon binding the large Ra^{2+} cation is counterbalanced by weaker dative interactions in the [Ra(macropa)] complex. Specifically, $E^{(2)}$ values increase from Ca^{2+} to Ba^{2+}, but then decrease for Ra^{2+}, which is qualitatively consistent with the experimental selectivity trend in Fig. 2a. Therefore, our DFT studies point to a subtle interplay between bonding interactions and molecular strain in defining the stability of Ra^{2+}–macrocycle complexes.

In summary, the aqueous complexation thermodynamics of Ra^{2+} were characterized with macropa and DOTA. Although both chelators exhibit high affinity for Ra^{2+} under Na^{+}-free, high-pH conditions, only macropa retains its affinity at pH 7.4, making it the highest affinity chelator reported for Ra^{2+} under physiologically relevant conditions. Our studies also revealed that macropa is not selective for Ra^{2+} over Ba^{2+}, despite its well-known ability to stabilize large metal ions. Our findings point to a delicate interplay between binding affinity, ligand basicity, metal-ion selectivity, and ligand strain that must be considered when designing new ligands to stabilize Ra^{2+}. Additionally, while Ba^{2+} is often used as a non-radioactive Ra^{2+} surrogate, our results show that Ra^{2+} chemistry cannot be simply predicted from Ba^{2+} behaviour under comparable circumstances. Although both thermodynamic and kinetic stabilities of complexes will dictate their ultimate stability in vivo, the insight garnered here into the thermodynamics of Ra^{2+} complexation relevant to TAT provides an important step towards establishing ligand design principles for the Ra^{2+} ion and enabling predictions of complex stability and speciation in biological media.

This research was supported by the U.S. DOE Isotope Program, managed by the Office of Science for Isotope R&D and Production, and by the Laboratory Directed Research and Development Program of ORNL. The staff of the Technical Services, Finishing, and Dispensing Group at ORNL are thanked for their isotope production and purification contributions. The manuscript was produced by UT-Battelle, LLC under Contract No. DE-AC05-00OR22725 with the U.S. Department of Energy. The publisher acknowledges the U.S. Government license to provide public access under the DOE Public Access Plan (http://energy.gov/downloads/doe-public-access-plan).

Conflicts of interest

There are no conflicts to declare.

Notes and references

1 (a) Y.-S. Kim and M. W. Brechbiel, *Tumor Biol.*, 2012, **33**, 573-590; (b) M. Makvandi, E. Dupis, J. W. Engle, F. M. Nortier, M. E. Fassbender, S. Simon, E. R. Birnbaum, R. W. Atcher, K. D. John, O. Rixe and J. P. Norenberg, *Target. Oncol.*, 2018, **13**, 189-203.

2 P. G. Kluetz, W. Pierce, V. E. Maher, H. Zhang, S. Tang, P. Song, Q. Liu, M. T. Haber, E. E. Leutzinger, A. Al-Hakim, W. Chen, T. Palmby, E. Alebachew, R. Sridhara, A. Ibrahim, R. Justice and R. Pazdur, *Clin. Cancer Res.*, 2014, **20**, 9-14.

3 M. W. Brechbiel, *Q. J. Nucl. Med. Mol. Imaging*, 2008, **52**, 166-173.

4 (a) X. Chen, M. Ji, D. R. Fisher and C. M. Wai, *Inorg. Chem.*, 1999, **38**, 5449-5452; (b) G. Henriksen, P. Hoff and R. H. Larsen, *Appl. Radiat. Isot.*, 2002, **56**, 667-671; (c) M. Gott, J. Steinbach and C. Mamat, *Open Chem.*, 2016, **14**, 118-129; (d) D. S. Abou, N. A. Thiele, N. T. Gutsche, A. Villmer, H. Zhang, J. J. Woods, K. E. Baidoo, F. E. Escorcia, J. J. Wilson and D. L. J. Thorek, *Chem. Sci.*, 2021, **12**, 3733-3742.

5 R. D. Shannon, *Acta Crystallogr. Sect. A*, 1976, **32**, 751-767.

6 P. L. Brown, A. V. Matyskin and C. Ekberg, *Radiochim. Acta*, 2022, DOI: 10.1515/ract-2021-1141.

7 (a) E. W. Price and C. Orvig, *Chem. Soc. Rev.*, 2014, **43**, 260-290; (b) E. Aluicio-Sarduy, N. A. Thiele, K. E. Martin, B. A. Vaughn, J. Devaraj, A. P. Olson, T. E. Barnhart, J. J. Wilson, E. Boros and J. W. Engle, *Chem. Eur. J.*, 2020, **26**, 1238-1242; (c) F. Reissig, D. Bauer, M. Ullrich, M. Kreller, J. Pietzsch, C. Mamat, K. Kopka, H.-J. Pietzsch and M. Walther, *Pharmaceuticals*, 2020, **13**, 272-272; (d) D. J. Fiszbein, V. Brown, N. A. Thiele, J. J. Woods, L. Wharton, S. N. MacMillan, V. Radchenko, C. F. Ramogida and J. J. Wilson, *Inorg. Chem.*, 2021, **60**, 9199-9211.

8 (a) N. A. Thiele, V. Brown, J. M. Kelly, A. Amor-Coarasa, U. Jermilova, S. N. MacMillan, A. Nikolopoulou, S. Ponnala, C. F. Ramogida, A. K. H. Robertson, C. Rodríguez-Rodríguez, P. Schaffer, C. Williams Jr, J. W. Babich, V. Radchenko and J. J. Wilson, *Angew. Chem. Int. Ed.*, 2017, **56**, 14712-14717; (b) N. A. Thiele and J. J. Wilson, *Cancer Biother. Radiopharm.*, 2018, **33**, 336-348.

9 M. Riondato, S. Pastorino, V. Duce, E. Giovannini and A. Ciarmiello, *Nucl. Med. Biol.*, 2019, **72-73**, S50-S51.

10 (a) J. Schubert, E. R. Russell and L. S. Myers, *J. Biol. Chem.*, 1950, **185**, 387-398; (b) J. Schubert, *J. Am. Chem. Soc.*, 1954, **76**, 3442-3444; (c) T. Sekine, Y. Kawashima, T. Unnai and M. Sakairi, *Bull. Chem. Soc. Jpn.*, 1968, **41**, 3013-3015; (d) Y. Shiokawa, T. Kido and S. Suzuki, *J. Radioanal. Nucl. Chem. Lett.*, 1985, **96**, 249-256; (e) A. V. Matyskin, N. L. Hansson, P. L. Brown and C. Ekberg, *J. Solution Chem.*, 2017, **46**, 1951-1969.

11 M. P. Jensen, R. Chiarizia, I. A. Shkrob, J. S. Ulicki, B. D. Spindler, D. J. Murphy, M. Hossain, A. Roca-Sabio, C. Platas-Iglesias, A. de Blas and T. Rodríguez-Blas, *Inorg. Chem.*, 2014, **53**, 6003-6012.

12 (a) J. Schubert, *J. Phys. Chem.*, 1948, **52**, 340-350; (b) J. Schubert and J. W. Richter, *J. Phys. Chem.*, 1948, **52**, 350-357.

13 K. L. Nash, *Radiochim. Acta*, 1991, **54**, 171-180.

14 S. M. Shanbhag and G. R. Choppin, *Inorg. Chem.*, 1982, **21**, 1696-1697.

15 G. Anderegg, F. Arnaud-Neu, R. Delgado, J. Felcman and K. Popov, *Pure Appl. Chem.*, 2005, **77**, 1445-1495.

16 J.-L. Burgot, in Ionic Equilibria in Analytical Chemistry, Springer, New York, 2012, pp. 485-501.

17 S. L. Wu and W. D. Horrocks, *J. Chem. Soc., Dalton Trans.*, 1997, 1497-1502.

18 (a) A. Roca-Sabio, M. Mato-Iglesias, D. Esteban-Gómez, É. Toth, A. de Blas, C. Platas-Iglesias and T. Rodríguez-Blas, *J. Am. Chem. Soc.*, 2009, **131**, 3331-3341; (b) R. Ferreirós-Martínez, D. Esteban-Gómez, É. Tóth, A. de Blas, C. Platas-Iglesias and T. Rodríguez-Blas, *Inorg. Chem.*, 2011, **50**, 3772-3784; (c) N. A. Thiele, S. N. MacMillan and J. J. Wilson, *J. Am. Chem. Soc.*, 2018, **140**, 17071-17078.

19 A. S. Ivanov and V. S. Bryantsev, *Eur. J. Inorg. Chem.*, 2016, **2016**, 3474-3479.